Electronic Supplementary Material

Label-free electrochemical aptasensor based on platinum@palladium nanoparticles decorated hemin- reduced graphene oxide as signal amplifier for glypican-3 determination

Guiyin Li[1,2#], Wenzhan Li[2#], Shengnan Li[2], Xinhao Li[2], Xiaoqing Yao[1], Wen Xue[3], Jintao Liang[2]*, Jiejing Chen[3*], Zhide Zhou[2]*

1. College of Chemistry, Guangdong University of Petrochemical Technology, Guandu Road, Maoming, Guangdong 525000, People's Republic of China
2. School of Life and Environmental Sciences, Guangxi Key Laboratory of Information Materials, Guilin University of Electronic Technology, Guilin, Guangxi 541004, People's Republic of China
3. Department of Clinical Laboratory, The 924st Hospital of Chinese People's Liberation Army Joint Logistic Support Force, Guangxi Key Laboratory of Metabolic Disease Research, Guilin, Guangxi 541002, China

[#] These authors contributed equally to this work.

*Corresponding author: dxljt@guet.edu.cn (J.T. Liang);

jiejingchen@126.com (J. J. Chen);

zhouzhide10@guet.edu.cn (Z.D. Zhou).

Tel: +86-773-2305206; Fax: +86-773-2305206

1. Characterization of H–rGO–Pt@Pd nanocomposites

TEM is used to reveal the morphology and structure of the prepared product. The TEM image (Fig. S1A) shows that the rGO has lamellar structure, H–rGO (Fig.S1B) are single layers, with random folds and curls.

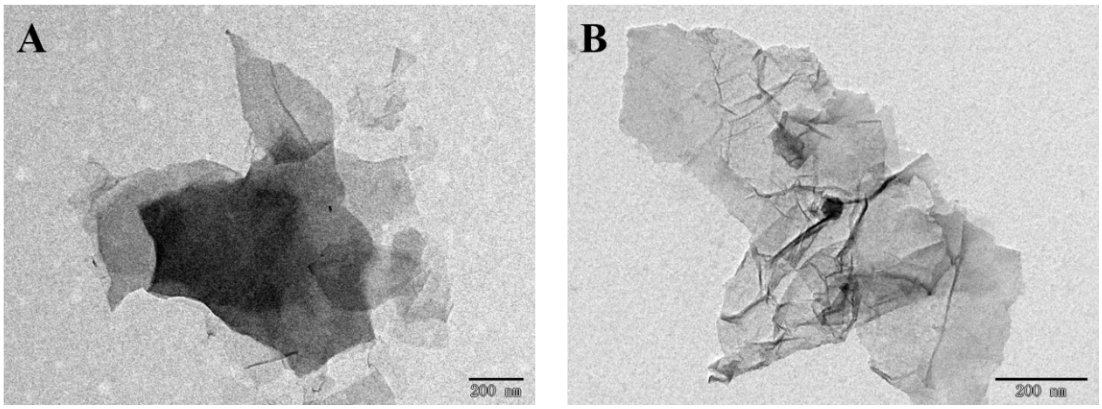

Fig. S1 TEM image of rGO (A) and H-rGO (B)

SEM is used to display the morphology of different materials. The SEM image (Fig. S2A) shows that the rGO surface is relatively flat, and the SEM image of (Fig. S2B) H–rGO shows a fold membrane-like structure pattern.

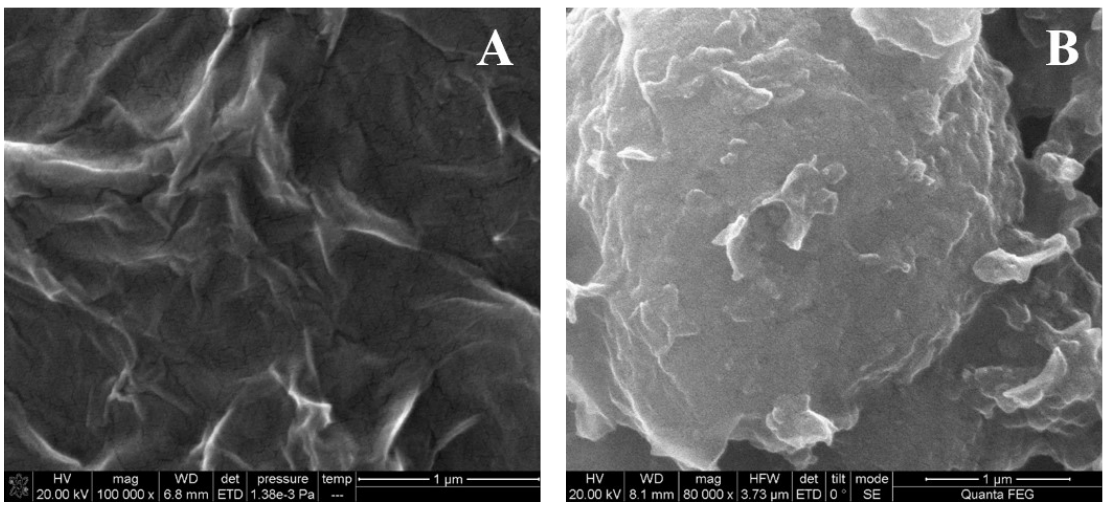

Fig. S2 SEM image of rGO (A) and H-rGO (B)

Fig.S3 is an analysis of the FT-IR of Heme (Fig.S3, Curve a), rGO (Fig.S3, Curve b), H-rGO (Fig.S3, Curve c), H-rGO-Pt@Pd NPs (Fig.S3, Curve d). Heme (Fig.S3, curve a) -OH telescopic vibration peak at 3425cm^{-1}, C=C vibration peak at 1630 cm^{-1}, 1384 cm^{-1} and 1087 cm^{-1} curves represent the peak vibration C-H and C-C. rGO (Fig.S3, curve b) −OH telescopic vibration peak at 3425cm^{-1}, C -C vibration peak at 1630 cm^{-1}, C-C vibration peak at 1107 cm^{-1}. H-rGO (Fig.S3, curve c), H-rGO-Pt@Pd NPs (Fig.S3, curve d) at 3425cm^{-1}, 1630 cm^{-1} and 1384 cm^{-1} respectively appeared the same -OH telescopic vibration peak, C=C vibration peak and C-H vibration peak, C-H vibration peak position change at 1116 cm^{-1} and 1076 cm^{-1}, C-H vibration peak position may be the offset caused by the binding of several materials, therefore, the above infrared spectral characterization results fully indicate the successful preparation of H-rGO-Pt@Pd NPs nanocomposite materials. The FT-IR of the H-rGO-Pt@Pd NPs is consistent with previous literature [1, 2].

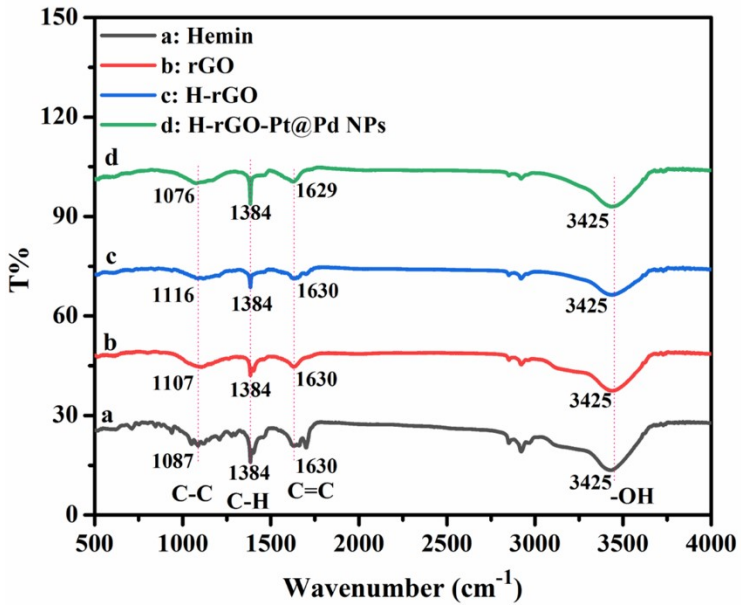

Fig.S3 The FT-IR of Heme (a), rGO (b), H-rGO (c)and H-rGO-Pt@Pd NPs(d).

2. Electrochemical performance of H–rGO–Pt@Pd NPs

CV method and EIS method are used to verify the function of the above different materials and the results are shown in Fig. S4. The CV scan of Au NPs/SPE (a), rGO/Au NPs/SPE (b), Pt@Pd NPs/Au NPs/SPE (c), rGO-Pt@Pd NPs/Au NPs/SPE (d), H-rGO-Pt@Pd NPs/Au NPs/SPE (e) was carried out in the voltage range from –1.0 V to +1.0 V with a scanning rate of 100 $mV \cdot s^{-1}$ in PBS solution (0.2 M, pH 6.0) including 5.0 mM $K_3Fe(CN)_6/K_4Fe(CN)_6$ and 0.1 M KCl. Besides, the EIS scan of the different electrodes mentioned above was measured in PBS solution (0.2 $mol \cdot L^{-1}$, pH 6.0) including 5.0 mM $K_3Fe(CN)_6/K_4Fe(CN)_6$ and 0.1 M KCl using the following parameters: direct current potential, 0.12 V; frequency range, 0.1 Hz and 10^5 Hz; amplitude, 5 mV. As seen from Fig. S4A, the current value of rGO/Au NPs/SPE is higher than that of the Au NPs/SPE. This is because rGO has excellent catalysis and conductivity, which enhances electron transfer efficiency. When Pt@Pd nanoparticles are incubated on the surface of Au NPs/SPE (Fig.S4A, curve c), the current peaks increase again because bimetal nanoparticles have better conductivity. After incubating rGO-Pt@Pd NPs on Au NPs/SPE, the oxidation peak current is further enhanced (Fig.S4a, curve d). This is because the bimetallic Pt@Pd NPs are combined with rGO, it can effectively prevent rGO from agglomerating, making rGO exert better performance. After the Au NPs/SPE electrode is incubated with H-rGO-Pt@Pd NPs (Fig.S4A, curve e), the current value reaches the maximum due to better conductivity of the H-rGO-Pt@Pd NPs.

The corresponding EIS scan is shown in Fig.S4B. When rGO is added dropwise, the Re value of rGO/Au NPs/SPE (Fig.S4B, curve b) is sharply reduced compared to Au NPs/SPE (Fig.S4B, curve a) due to the large surface of rGO and thus facilitating the electron transfer. When replacing rGO with the bimetallic Pt@Pd NPs, the Re value of Pt@Pd NPs/Au NPs/SPE (Fig.S4B, curve c) is smaller than that of rGO/Au NPs/SPE

due to the excellent conductivity of the bimetal. Since the electrode has both rGO with large specific surface area and bimetal with excellent conductivity, the Re value of rGO-Pt@Pd NPs/Au NPs/SPE (Fig.S4B, curve d) is reduced. Further, when replacing rGO-Pt@Pd NPs with H-rGO-Pt@Pd NPs, the Re value of H-rGO-Pt@Pd NPs/Au NPs/SPE (Fig.S4B, curve e) become smaller due to the increased catalytic performance of Hemin.

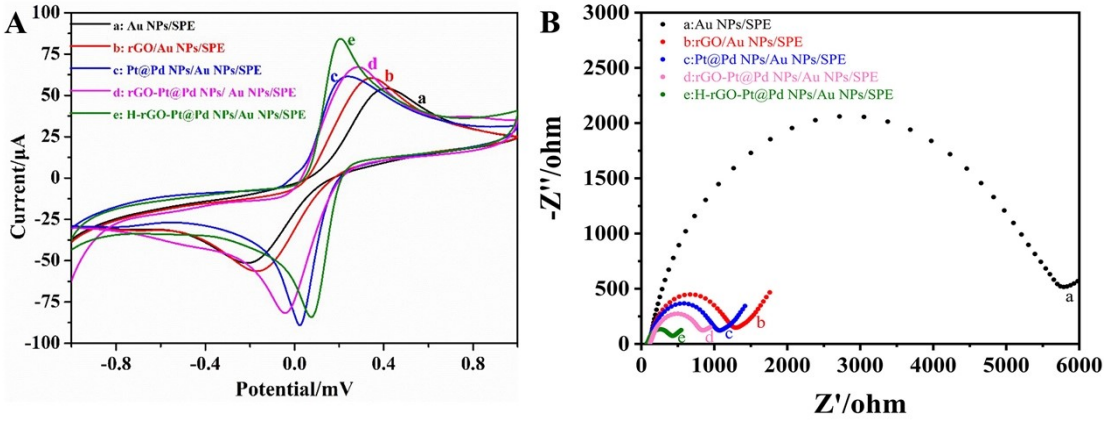

Fig.S4 The (A) CV graph and (B) EIS graph of Au NPs/SPE (a), rGO/Au NPs/SPE (b), Pt@Pd NPs/Au NPs/SPE (c), rGO-Pt@Pd NPs/Au NPs/SPE(d), H-rGO-Pt@Pd NPs/Au NPs/SPE (e).

3. Optimization of experimental conditions

For the sake of achieving the best sensing performance, some key experimental conditions have been optimized including the concentrations of H–rGO–Pt@Pd NPs composites and the GPC3 aptamer, the incubation time and the temperature of GPC3, the pH of PBS solution are evaluated. All the results are shown in Fig.S5.

Fig. S5A shows the current change of GPC3 incubation temperature between 4°C to 37°C. This is due to the fact that incubation temperature affects the protein activity and thus the binding between the aptamer and the protein. It can be seen that the DPV peak current increases first and then decreases. And the current response is maximum

at 15°C (1.922 μA). Suitable temperature increases the $GPC3_{Apt}$-GPC3 binding rate, increases $GPC3_{Apt}$-GPC3 complexes taken away by washing, and increases the current. Therefore, 15°C is the optimal incubation temperature for GPC3.

Fig. S5B is the optimization of H–rGO–Pt@Pd NPs concentration. The change in the DPV peak current increases from 0.1 $mg \cdot mL^{-1}$ to 0.2 $mg \cdot mL^{-1}$, and then decreases gradually from 0.2 $mg \cdot mL^{-1}$ to 0.5 $mg \cdot mL^{-1}$. The current peak is maximum (2.116 μA) when the composite concentration is 0.2 $mg \cdot mL^{-1}$, suggesting that the H–rGO–Pt@Pd NPs composites reached saturation on the surface of Au NPs/SPE. It could be due to a larger surface area and higher conductivity. On the other hand, at a higher concentration (higher than 0.2 $mg \cdot mL^{-1}$), a significant decrease in current occurs due to a decrease in the exposed electroactive surface area and a slowing down of the electron transfer rate as the adsorption sites on the material surface area covered or aggregated. Therefore, 0.2 $mg \cdot mL^{-1}$ is used for the follow-up experiments.

Fig. S5C shows the optimization of $GPC3_{Apt}$ concentration. With a slight decrease in the concentration of $GPC3_{Apt}$ from 0.5 $\mu mol \cdot L^{-1}$ to 1.0 $\mu mol \cdot L^{-1}$, the peak current increases from 1.0 $\mu mol \cdot L^{-1}$ to 3.0 $\mu mol \cdot L^{-1}$ and reached a maximum at 3.0 $\mu mol \cdot L^{-1}$ (2.678 μA), and then the peak current from 3.0 $\mu mol \cdot L^{-1}$ to 10.0 $\mu mol \cdot L^{-1}$ is gradually reduced to a stable state. The result reveals that excessive $GPC3_{Apt}$ concentration can cover the electroactive sites on the surface of the material resulting in reduced effective area for electron transfer and lower current. As can be seen from this, 3.0 $\mu mol \cdot L^{-1}$ is the optimal concentration of $GPC3_{Apt}$.

Fig. S5D depicts the optimization of incubation reaction time for GPC3 and $GPC3_{Apt}$ in order to ensure sufficient time for antigen GPC3 and $GPC3_{Apt}$ binding and to generate the maximum current response signal. The peak current increases slightly from 10 min to 20 min, from 20 min to 40 min, from 40 min to 60 min, then reaches

the maximum value (2.793 μA) within 60 min, and gradually decreases from 60 min to 120 min. The results show that the formation of the GPC3-$GPC3_{Apt}$ complex is completed after 60 min. Therefore, 60 min is the best incubation time for GPC3 and $GPC3_{Apt}$.

Fig.S5E shows the optimal pH of PBS solution. This is due to the pH will affect the activity of the GPC3 protein, thus the response signal. The peak current increases significantly with the pH increase from 5.5 to 6.0, and then reaches the maximum value at 6.0 (14.6 μA). The peak current gradually reduced from 6.0 to 7.5. It turns out that 6.0 is the optimal pH of PBS solution.

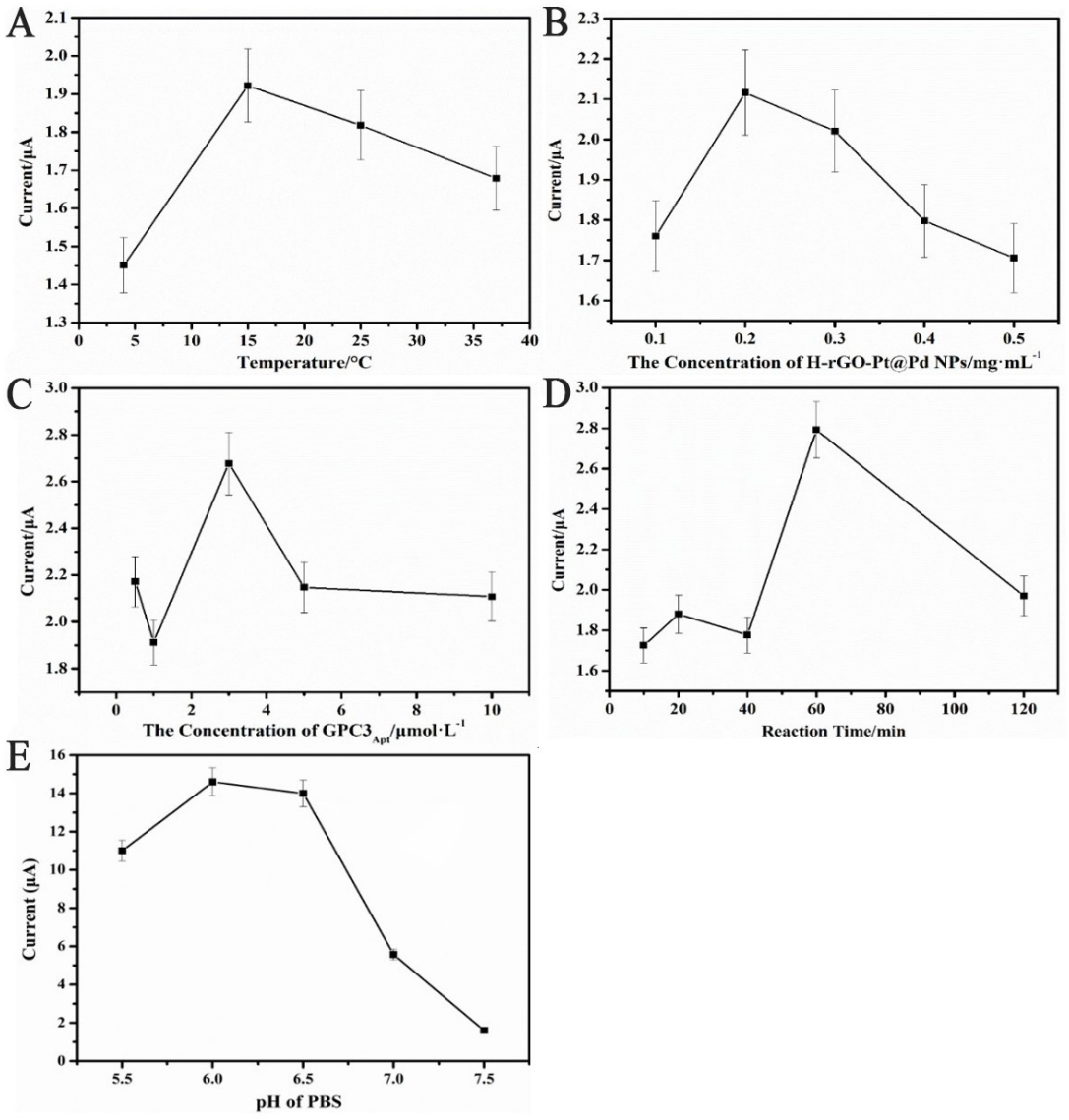

Fig.S5 Optimization of (A) Incubation temperature, (B) Concentration of the H–rGO–Pt@Pd NPs, (C) Concentration of $GPC3_{Apt}$, (D) Incubation time, (E) pH value of PBS, by using 10.0 $\mu g \cdot mL^{-1}$ GPC3 as an example. All the above values are expressed as the median of three independent analyses, the error bar represents the relative standard deviation from three independent measurements.

Reference

[1] S. Esabattina, V.R. Posa, H. Zhanglian, S.k. Godlaveeti, R.R. Nagi Reddy, and A.R. Somala, Fabrication of bimetallic PtPd alloy nanospheres supported on rGO sheets for superior methanol electro-oxidation, Int. J. Hydrogen Energy, 43 (2018) 4115-4124. https://doi.org/10.1016/j.ijhydene.2017.07.193.

[2] G. Vishwakshan Reddy, P. Raghavendra, P. Sri Chandana, and L. Subramanyam Sarma, Halide-aided controlled fabrication of Pt–Pd/graphene bimetallic nanocomposites for methanol electrooxidation, RSC Advances, 5 (2015) 100522-100530. https://doi.org/10.1039/c5ra14682h.